Analyzing Fluid Shear Stress in the RCCS: Applications for 3D Cell Culture in Simulated Microgravity.

T. Masiello*[1], A. Dhall[1], M. Hemachandra[1], N. Tokranova[1], JA. Melendez[1], J. Castracane[1]
[1]SUNY Polytechnic Institute, Colleges of Nanoscale Science and Engineering, Albany, NY, USA
*Corresponding author: SUNY Polytechnic Institute, Nanobioscience Constellation, 257 Fuller Rd, Albany, NY 12203. Email: tmasiello@sunypoly.edu

Introduction

In the decades since humans first went to space, there has been growing interest in utilizing microgravity to improve our understanding in many scientific fields (1). Applied fields have included evolutionary development, cell mechanics and protein crystallization (2-4). The scientific potential is undeniable; more than 1500 experiments have been conducted on the International Space Station (ISS) over the past 15+ years, resulting in over 60 publications (5). The number of microgravity-related parents has grown steadily over the past thirty years as well (6).

Microgravity offers an unprecedented opportunity for the isolation of gravity as an experimental variable to elucidate cellular pathways, behaviors and attributes otherwise inaccessible that might be applied to benefit areas such as drug development, disease studies and tissue engineering. Among the most notable observations, in terms of impact on human health, is that expressions of metastatic markers were reduced in several kinds of cancer cell lines upon exposure to microgravity (7, 8). However, it is not yet known if the overall metastatic/cancerous potential of these cells *in vivo* is decreased. Understanding the mechanisms/pathways behind such changes could lead to discovery of new therapeutic signaling pathways and their potential targets for delaying or preventing cancer metastasis.

Performing experiments in microgravity, such as aboard the ISS, is a long, expensive and challenging process. Thus, the foundation for those ventures is typically laid using Earth-based simulation methods. These include the Random Positioning Machine (RPM), parabolic flight and, of interest here, the Rotary Cell Culture System (RCCS) developed by NASA and produced by Synthecon™, shown in Figure 1 (9). The horizontally-oriented High Aspect Ratio Vessels (HARVs) create a low-shear stress environment for three-dimensional (3D) culture of cells, producing cell aggregates called spheroids (10). 3D cell culture is becoming an increasingly prominent tool for tumor biology, among other fields, as spheroids are commonly used as tumor models for breast cancer, among others (11), and are specifically a crucial part of transcoelomic metastasis in ovarian cancer (12). Examples of cancer spheroids formed in the RCCS are shown in Figure 2, showing both round and irregular morphologies for different cell lines.

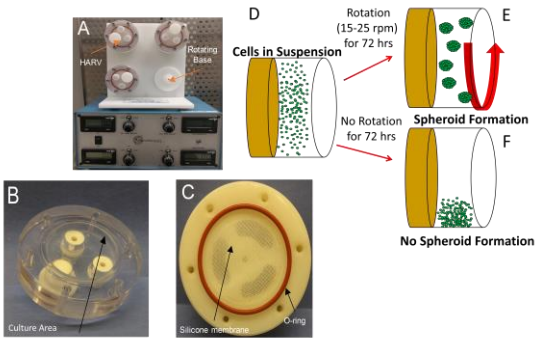

Figure 1. The RCCS and its schematic of operations. A) The main body of the RCCS with the controller (bottom box) and three HARVs attached to the rotating bases. B,C) The two main components of the HARV, both the front with syringe fill ports and culture area (B) and the back with a silicone membrane for oxygen exchange (C). D) A suspension of cells is placed in the HARV and will either form spheroids over time if rotated (E) or the cells will pool at the bottom and not form spheroids if the rotation is absent (F).

The forces acting on cells/spheroids within HARVs have been analyzed mathematically before but most studies focused on specific assumed parameters, typically rotation speed and aggregate size (13). The Computational Fluid Dynamics (CFD) module and Particle Tracing module of COMSOL® Multiphysics can be used to analyze the shear stresses produced in HARVs and model the positions of spheroids within them. It is important, however, to account for different cell types forming spheroids of varying sizes, which will behave differently under identical rotating conditions due to their greater mass and surface area. To resolve this, the shear stress will be adjusted by modifying the rotation speed and the viscosity of the culture media. This will help maintain the consistency of simulated microgravity experiments

across different cell types, improving the quality and consistency of simulated microgravity experiments.

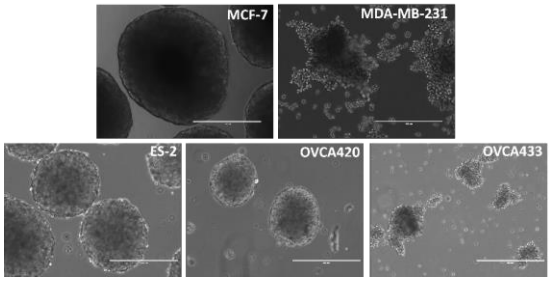

Figure 2. Representative images of spheroids generated in the RCCS at a cell density of $1x10^5$ cells/mL over 72 hrs with a ramped rotation of 15-25 rpm. This includes both breast cancer **(**MCF-7 and MDA-MB-231) and ovarian cancer cell lines (ES-2, OVCA420, and OVCA433). Scale Bar: 400 μm.

Governing Equations

For incompressible, single phase flow under laminar conditions, and following the Navier-Stokes equation, the velocity of the fluid was determined using the following equations:

Equation 1

$$\rho(u \cdot \nabla)u = \nabla \cdot [-\rho I + \mu(\nabla u + (\nabla u)^T)] + F + \rho g$$

$$\rho \nabla \cdot (u) = 0$$

Shear stress over the area of the HARV was calculated by averaging the shear stress in the x,y and z directions using the following equation:

Equation 2 (14)

$$WSS = \sqrt{\tau^2{}_{xy} + \tau^2{}_{yz} + \tau^2{}_{xz}}$$

The nomenclature section lists the symbols used in these equations.

Methods

Two types of simulation studies were conducted – A single phase flow study under laminar conditions for the flow of media with the HARV and a particle tracing study to monitor the trajectory of spheroids under the flow of media. All simulations used a physics-controlled mesh with normal element size.

Single Phase Flow (spf)

Spf studies under laminar conditions were run with using cell media as the fluid within a HARV. The size of the HARV was constant so the variables were the rotating speed and the viscosity of the media. The HARV used here has a 10 mL volume with a diameter of 4.5 cm and a height of 0.63 cm. Cell culture media in its base formulation has a density and viscosity nearly identical to water. The viscosity can be easily altered by adding serum or a polymer additive. Starting values of viscosity and density of media at 37 ºC are 0.69 cP and 0.9933 g/cm^3 respectively. Based on Equation 1, increasing the viscosity will decrease the velocity of the spheroids and thus decrease the shear stress. The viscosity will be hypothetically altered using methyl cellulose, a readily-available and biocompatible polymer already used for such experiments as aiding spheroid formation in hanging drops (15).

The chosen rotation speeds for the RCCS were 15 and 25 rpm, representing both typical speeds in the literature (16, 17) and our own optimization experiments. A rotating domain was defined in the clockwise direction along the z-axis to mimic the horizontal orientation of HARVs on the RCCS. Simulation results included both velocity distributions and shear stress calculations based on the above equation. This was repeated for 3 different viscosity values: 0.75 cP (mimicking complete growth media with serum (18), 1.0 cP and 1.25 cP (mimicking methyl cellulose concentrations of 0.5% and 0.625% respectively).

Particle Tracing

Particle sizes were chosen based on both spheroids we have generated in the RCCS and in the range of what has been previously published (19). The particle mass was calculated based on the volume of the spheroid and an assumed density of 1.04 g/cm^3, similar to previous studies (20).

Cell Culture

Breast cancer cell lines MCF-7 and MDA-MB-231 were grown in Dulbecco's Modified Eagle Medium (DMEM). Ovarian cancer cell lines OVCA420 and OVCA433, as well as the non-cancer NOSE007, were maintained in RPMI 1640 media while ES-2 cells were maintained in McCoy's 5A (modified) media. Each media formulation was supplemented with 10% fetal bovine serum (FBS) and 1% penicillin/streptomycin. All cells were grown in an incubator at 37°C and under a 5% CO_2 and 95% air atmosphere. Cell passaging was performed every 2-3 days using 0.05% trypsin/EDTA. Cells were passaged no more than 6 times after thawing.

Simulation of Microgravity using the RCCS

Cells were passaged as described above and seeded in 10 mL HARVs at a final density of 1 x10^5 cells/mL. The volume was adjusted to completely fill the vessel and remove all air bubbles using syringes. Air bubbles were also removed as needed over the culture period. HARVs were rotated on the RCCS with a starting rotation of 15 rpm. This was increased by 5 rpm every 24 hrs up to a speed of 25 rpm to account for the increase in spheroid size (9). After 72 hours the spheroids were collected by gentle pipetting. If culturing proceeded beyond 72 hrs, roughly two-thirds of the media was exchanged at 72 hrs and every 48 hrs thereafter while the rotation was kept constant at 25 rpm. All spheroid images were taken on an eVOSfl AMG LED-based fluorescent microscope and size measurements were taken using ImageJ.

Results

Initial CFD simulations were run to measure the base fluid shear stress with no particles present. Typical speeds for the RCCS range from 10-30 rpm (21). The spheroids shown in Figure 2 were generated as described above with a ramped rotation rate. The simulations in Figure 3 show a difference of about one order of magnitude in the shear stress going from 15 rpm to 25 rpm. This assumes a fluid viscosity of 0.75 cP, consistent with complete cell growth media. The values (~10^{-4}-10^{-5} dPa) fall within the range of physiological shear stresses, which can vary from below 0.1 dPa to above 10 (22).

With baseline parameters established particle tracing experiments were run using particle radii of 50, 100 and 200 µm, covering a wide size range of

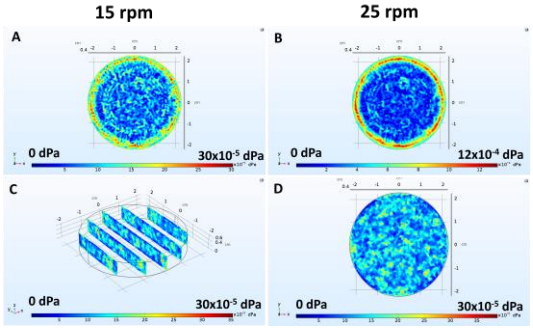

Figure 3. Baseline fluid shear stress at the top of a HARV at 15 (A) and 25 rpm (B). The highest shear stress is at the edges of the HARV. C) Cross-sectional slices of shear stress distribution at 15 rpm. D) Fluid shear stress in the middle of the HARV.

spheroids. Figure 4 shows that at 15 rpm the smallest particles are pushed to the edges of the HARV while the 100 µm and 200 µm particles are continuously suspended in the middle of the HARV, rotating as expected under the balance of Coriolis, centrifugal and a reduced gravitational force (23). At 25 rpm the results for the 50 and 200 µm particles are nearly identical in positioning but the 100 µm particles have moved closer to the edges of the HARV and away from the center. This suggests the higher rotation speed is pushing the spheroids tend towards the high stress area of the HARV edges.

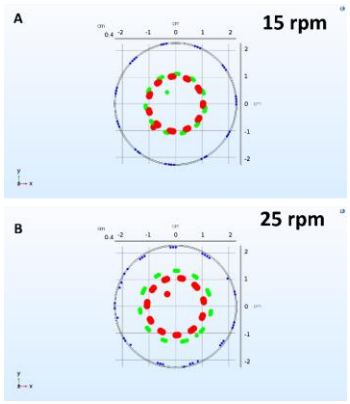

Figure 4. Particle Tracing of Spheroids at 15 (A) and 25 rpm (B). Particles were 50 (blue), 100 (green) and 200 (red) µm in radius. In both cases the smallest spheroids are readily deflected to the outer edges of the HARVs while the larger, heavier particles tend towards the middle.

If experiments across various spheroid sizes are to be consistent, the spheroids must be encouraged

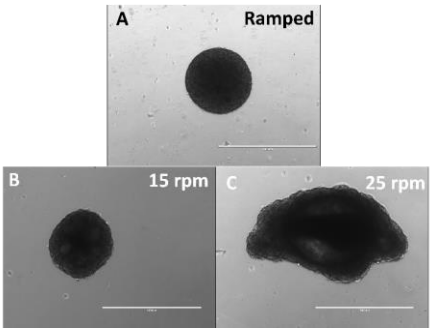

Figure 5. The effects of constant rotation speed on MCF-7 spheroid formation. A) Spheroid formed under ramped rotating conditions (5 rpm every 24 hrs, starting from 15 rpm up to 25 rpm) for 72 hrs. B) Spheroids formed under constant 15 rpm for 72 hrs have nearly identical morphology to ramped rotation. C) Spheroids formed under constant 25 rpm for 72 hrs show irregular, misshapen morphology. Scale bar: 1000 µm.

to follow similar patterns of flow as deviations can alter behavior. The effects of increased shear stress on spheroid formation are shown in Figure 5, where MCF-7 spheroids were formed under constant speeds of 15 and 25 rpm. While the 15 rpm spheroids are quite similar to those formed under the previously-described ramped speed the spheroid morphology becomes more irregular at 25 rpm compared to normal MCF-7 spheroids (24). It is possible that these spheroids are forming more quickly and becoming larger faster under 25 rpm, and their morphology alters under prolonged exposure to high shear stress past the initial

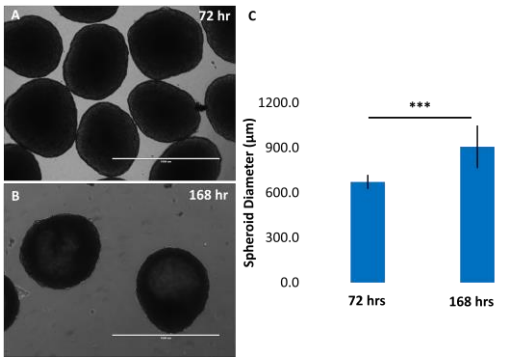

Figure 6. Spheroid size increases for long-term RCCS culture. MCF-7 were spheroids formed under established rotating conditions for A) 72 hrs and B) 168 hrs. Scale Bar: 1000 µm. C) The average spheroid diameter rises from 672 µm to 906 µm. Error bars represent standard deviation, p value < 10^{-3}.

spheroid formation. Another example is when experiments are long-term, and the longer proliferation time causes an increase in spheroid size. Figure 6 shows this size change for MCF-7 spheroids cultured for 168 hrs instead of 72 hrs. This can create an unintended increase in shear stress over the course of the experiment and skew the results.

While changing the rotation speed is the simplest way to affect the shear stress it is limited by the conditions for simulating microgravity. As mentioned earlier, there must be balance between the Coriolis and centrifugal forces. An alternate way to alter the shear stress without compromising this balance is to increase the viscosity of the media. This is a common practice in various cell culture techniques, including for spheroid formation in hanging drop methods, where the viscosity is modulated by the addition of biopolymers such as methyl cellulose and dextran (15). These do not reduce viability or dramatically alter cell behavior, making them ideal choices for such experiments. New baseline fluid shear stress simulations were run using two increased values of viscosity: 1.0 cP and 1.25 cP. The

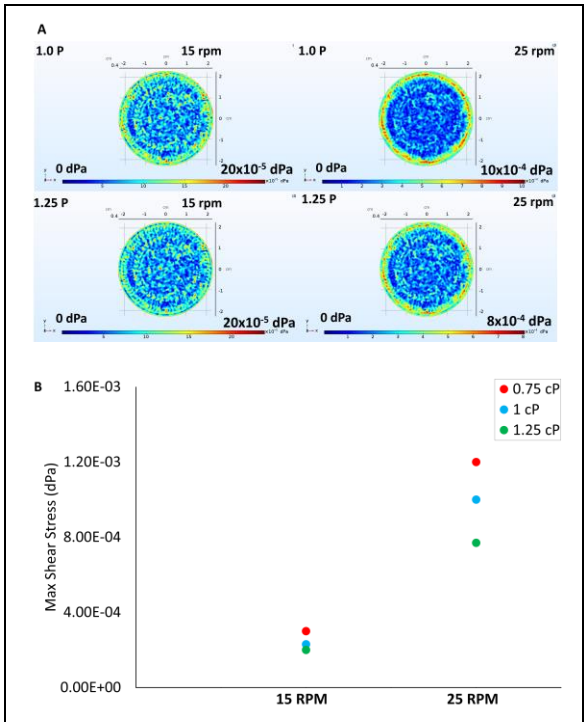

Figure 7. The Effects of Viscosity on Shear Stress. A) CFD simulations of shear stresses at both 15 rpm and 25 rpm for both 1.0 and 1.25 cP at the top of the HARV. The range of maximum shear stress is graphed in B. There is comparatively little difference between the two viscosities as opposed to the two rotation speeds.

change in the max shear stress is graphed in Figure 7, showing that while the difference between 15 and 25 rpm the difference in shear stress is still an order of magnitude, there is noticeably less difference between the two viscosities at either speed. As a follow-up, particle tracing experiments were repeated under these increased viscosities and Figure 8 shows how the 100 µm particles see a decrease in their relative distance from the center of the HARV, keeping their position closer to what is seen at 15 rpm.

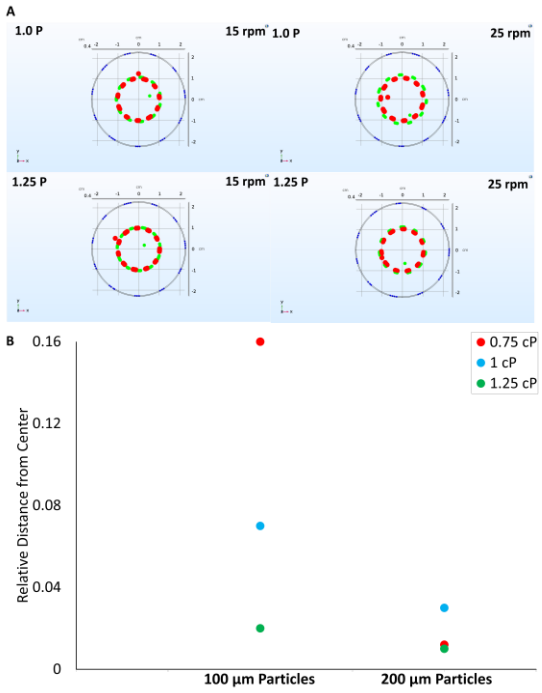

Figure 8. The Effects of Viscosity on Spheroid Position. A) Particle tracing simulations of spheroid position at both 15 rpm and 25 rpm for both 1.0 and 1.25 P. The relative distance from the center at 25 rpm is quantified in B. The differences between positions of 50 and 200 µm spheroids are minor but for 100 µm the deviation from the middle at 25 rpm is considerably restored by increasing the viscosity.

Conclusions

Microgravity has enormous potential to enhance our understanding in many areas of biology. The development of such experiments utilizing spheroids for studies on a platform such as the ISS can depend on the consistency and dependability of simulated microgravity experiments. CFD experiments show the low shear stress within HARVs and particle tracing models how the spheroids behave under that shear stress. This also illustrates how under higher rotation speeds spheroids of certain sizes may drift away from the low-shear stress center of the HARV, and RCCS experiments reinforce how such deviations can affect spheroid properties. However, they also show how modulating the media viscosity could lead to improved consistency of experiments over various sizes of spheroids as the spheroids are no longer pushed towards the higher-stress edges of the HARV.

None of the conditions tested here improved the spheroid position/shear stress experienced by the smallest particles. Microgravity conditions tend to promote the formation of large spheroids, some above 1 mm in diameter (25), so this is not expected to be a significant concern. If smaller spheroids are needed, though, there are ways to address this by using higher methyl cellulose concentrations or higher-diameter HARVs to create more low-shear stress areas.

Further simulations will model a time-course of the change in spheroid position in the first 72 hrs. It is during this time that individual cells aggregate and proliferate, increasing in size rapidly. This will continue into the long-term culture where the spheroid size continues to increase. Additionally, RCCS experiments and subsequent spheroid characterization using methyl cellulose-supplemented media will verify and complement the simulation data. All of these studies will be further applied to spheroids of other cell types, expanding on the versatility of the RCCS as an on-ground microgravity simulator and its ability to create physiologically-relevant shear stress.

Acknowledgements

We would like to thank our collaborators at SpacePharma Inc. for their advice. This project was funded by the Office of the Chief Scientist (Israel) and SUNY Polytechnic Institute.

Nomenclature

ρ Fluid density
g Acceleration due to gravity
u Flow velocity
µ Dynamic viscosity
F External force
τ Shear stress
WSS Wall shear stress

References

1. Hughes-Fulford M. To infinity ... and beyond! Human spaceflight and life science. FASEB

J. 2011;25(9):2858-64. doi: 10.1096/fj.11-0902ufm. PubMed PMID: 21880668.
2. Marco R, Diaz C, Benguria A, Mateos J, Mas J, de Juan E. The role of gravity in the evolutionary emergence of multicellular complexity: Microgravity effects on arthropod development and aging. Advances in Space Research. 1999;23(12):2075-82.
3. Janmaleki M, Pachenari M, Seyedpour SM, Shahghadami R, Sanati-Nezhad A. Impact of Simulated Microgravity on Cytoskeleton and Viscoelastic Properties of Endothelial Cell. Sci Rep. 2016;6:32418. doi: 10.1038/srep32418. PubMed PMID: 27581365; PMCID: PMC5007526.
4. Stelian C, Duffar T. Influence of rotating magnetic fields on THM growth of CdZnTe crystals under microgravity and ground conditions. Journal of Crystal Growth. 2015;429:19-26. doi: 10.1016/j.jcrysgro.2015.07.034.
5. NASA. International Space Station Utilization Statistics, Expeditions 0-32, December 1998 – September 20122013.
6. Uhran ML, editor. Microgravity-related patent history. 1st Annual International Space Station Research & Development Conference, Denver, CO; 2012.
7. Vidyasekar P, Shyamsunder P, Arun R, Santhakumar R, Kapadia NK, Kumar R, Verma RS. Genome Wide Expression Profiling of Cancer Cell Lines Cultured in Microgravity Reveals Significant Dysregulation of Cell Cycle and MicroRNA Gene Networks. PLoS One. 2015;10(8):e0135958. doi: 10.1371/journal.pone.0135958. PubMed PMID: 26295583; PMCID: PMC4546578.
8. Takeda M, Magaki T, Okazaki T, Kawahara Y, Manabe T, Yuge L, Kurisu K. Effects of simulated microgravity on proliferation and chemosensitivity in malignant glioma cells. Neurosci Lett. 2009;463(1):54-9. doi: 10.1016/j.neulet.2009.07.045. PubMed PMID: 19628020.
9. Barzegari A, Saei AA. An update to space biomedical research: tissue engineering in microgravity bioreactors. Bioimpacts. 2012;2(1):23-32. doi: 10.5681/bi.2012.003. PubMed PMID: 23678438; PMCID: PMC3648913.
10. Goodwin T, Prewett T, Wolf DA, Spaulding G. Reduced shear stress: A major component in the ability of mammalian tissues to form three-dimensional assemblies in simulated microgravity. Journal of cellular biochemistry. 1993;51(3):301-11.
11. Weiswald LB, Bellet D, Dangles-Marie V. Spherical cancer models in tumor biology. Neoplasia. 2015;17(1):1-15. doi: 10.1016/j.neo.2014.12.004. PubMed PMID: 25622895; PMCID: PMC4309685.
12. Shield K, Ackland ML, Ahmed N, Rice GE. Multicellular spheroids in ovarian cancer metastases: Biology and pathology. Gynecol Oncol. 2009;113(1):143-8. doi: 10.1016/j.ygyno.2008.11.032. PubMed PMID: 19135710.
13. Liu T, Li X, Sun X, Ma X, Cui Z. Analysis on forces and movement of cultivated particles in a rotating wall vessel bioreactor. Biochemical engineering journal. 2004;18(2):97-104.
14. Gutierrez RA, Crumpler ET. Potential effect of geometry on wall shear stress distribution across scaffold surfaces. Ann Biomed Eng. 2008;36(1):77-85. doi: 10.1007/s10439-007-9396-5. PubMed PMID: 17963042.
15. Matak D, Brodaczewska KK, Lipiec M, Szymanski L, Szczylik C, Czarnecka AM. Colony, hanging drop, and methyl cellulose three dimensional hypoxic growth optimization of renal cell carcinoma cell lines. Cytotechnology. 2017;69(4):565-78. doi: 10.1007/s10616-016-0063-2. PubMed PMID: 28321776; PMCID: PMC5507837.
16. Frith JE, Thomson B, Genever PG. Dynamic three-dimensional culture methods enhance mesenchymal stem cell properties and increase therapeutic potential. Tissue Engineering Part C: Methods. 2009;16(4):735-49.
17. Zheng H-x, Tian W-m, Yan H-j, Jiang H-d, Liu S-s, Yue L, Han F, Wei L-j, Chen X-b, Li Y. Expression of estrogen receptor α in human breast cancer cells regulates mitochondrial oxidative stress under simulated microgravity. Advances in Space Research. 2012;49(10):1432-40. doi: 10.1016/j.asr.2012.02.020.
18. Wang C, Lu H, Schwartz MA. A novel in vitro flow system for changing flow direction on endothelial cells. J Biomech. 2012;45(7):1212-8. doi: 10.1016/j.jbiomech.2012.01.045. PubMed PMID: 22386042; PMCID: PMC3327813.
19. Zhang S, Zhang Y, Chen L, Liu T, Li Y, Wang Y, Geng Y. Efficient large-scale generation of functional hepatocytes from mouse embryonic stem cells grown in a rotating bioreactor with exogenous growth factors and hormones. Stem cell research & therapy. 2013;4(6):1.
20. Tsao Y-MD, Boyd E, Wolf DA, Spaulding G. Fluid dynamics within a rotating bioreactor in space and earth environments. Journal of Spacecraft and Rockets. 1994;31(6):937-43.
21. Begley CM, Kleis SJ. The fluid dynamic and shear environment in the NASA/JSC rotating-wall perfused-vessel bioreactor. Biotechnology and bioengineering. 2000;70(1):32-40.
22. Regmi S, Fu A, Luo KQ. High Shear Stresses under Exercise Condition Destroy Circulating Tumor Cells in a Microfluidic System. Sci Rep. 2017;7:39975. doi: 10.1038/srep39975. PubMed PMID: 28054593; PMCID: PMC5215453.

23. Hammond T, Hammond J. Optimized suspension culture: the rotating-wall vessel. American Journal of Physiology-Renal Physiology. 2001;281(1):F12-F25.
24. Zhang W, Li C, Baguley BC, Zhou F, Zhou W, Shaw JP, Wang Z, Wu Z, Liu J. Optimization of the formation of embedded multicellular spheroids of MCF-7 cells: How to reliably produce a biomimetic 3D model. Anal Biochem. 2016;515:47-54. doi: 10.1016/j.ab.2016.10.004. PubMed PMID: 27717854.
25. Pietsch J, Ma X, Wehland M, Aleshcheva G, Schwarzwalder A, Segerer J, Birlem M, Horn A, Bauer J, Infanger M, Grimm D. Spheroid formation of human thyroid cancer cells in an automated culturing system during the Shenzhou-8 Space mission. Biomaterials. 2013;34(31):7694-705. doi: 10.1016/j.biomaterials.2013.06.054. PubMed PMID: 23866977.